Superconductor
Science and
Technology

PAPER • **OPEN ACCESS**

Analysing the RF & IF bandwidth performances of ALMA Band-9 superconducting mixers for wideband sensitivity upgrade

To cite this article: B-K Tan *et al* 2025 *Supercond. Sci. Technol.* **38** 085001

OPEN ACCESS
IOP Publishing
Superconductor Science and Technology
Supercond. Sci. Technol. **38** (2025) 085001 (12pp)
https://doi.org/10.1088/1361-6668/adea63

Analysing the RF & IF bandwidth performances of ALMA Band-9 superconducting mixers for wideband sensitivity upgrade

B-K Tan[1,*], J-H Kim[1], C Chaumont[2], F Boussaha[2] and A Baryshev[3]

[1] Department of Physics (Astrophysics), University of Oxford, DWB Keble Road, OX1 3RH Oxford, United Kingdom
[2] LUX, Observatoire de Paris, Université PSL, Sorbonne Université, CNRS, 75014 Paris, France
[3] Kapteyn Astronomical Institute, University of Groningen, 9747 AD Groningen, The Netherlands

E-mail: boonkok.tan@physics.ox.ac.uk

Received 6 February 2025, revised 15 April 2025
Accepted for publication 30 June 2025
Published 28 July 2025

Abstract

The Atacama Large Millimetre/Sub-millimetre Array (ALMA) wideband sensitivity upgrade (WSU) project marks the next milestone in the development of millimetre (mm) and sub-mm astronomy. In this paper, we present the design, optimisation, and performance analysis of the ALMA Band-9 superconductor-insulator-superconductor (SIS) mixer for applications in the upcoming WSU programme, and other high-frequency astronomical observations. The mixers feature a niobium radial-rectangular probe antenna integrated with a silicon-on-insulator (SOI) substrate, which ensures minimal RF power leakage and optimised power coupling. We base our mixer design on conventional aluminium oxide (AlO_x) tunnel junction technology, with a critical current density of about 10 kA cm^{-2}. We explore the impact of different junction sizes on the radio frequency (RF) and intermediate frequency (IF) bandwidths. We demonstrate that the new mixer design is capable of meeting the more stringent sensitivity-bandwidth requirements of the ALMA-WSU programme over the original Band-9 frequency range (602–720 GHz), as the IF bandwidth performance reaches up to 20 GHz. The IF bandwidth improvement is approximately double that of the current existing ALMA Band-9 mixers. These results suggest that our mixer designs provide a promising solution for future ALMA upgrades and other high-frequency applications requiring broad RF and IF bandwidth.

Keywords: superconductor-insulator-superconductor (SIS), heterodyne mixers, Atacama Large Millimetre/sub-millimetre Array, broadband, niobium transmission line, aluminium oxide junctions

* Author to whom any correspondence should be addressed.

1. Introduction

It has become customary to define the millimetre (mm) and sub-millimetre (sub-mm) observational windows, spanning the frequency range from 30 GHz to 1 THz, based on the atmospheric conditions in the Atacama Desert, where the Atacama Large Millimetre/sub-millimetre Array (ALMA) is located. However, only a few exceptionally high and dry sites, such as the Atacama Desert and the summit of Hawai'i Island, are capable of supporting observations across this extensive frequency range.

Within this mm/sub-mm range, a clear demarcation occurs near 350 GHz, corresponding to the boundary between ALMA-defined Band-7 and Band-8. Observing conditions beyond this frequency limit are particularly challenging for most ground-based telescopes due to atmospheric constraints. Consequently, space-borne or balloon-based missions are often required to overcome these limitations. This higher frequency range includes Band-9 (602–720 GHz), which is of particular significance as it encompasses the critical carbon monoxide (CO) $J = 6 \rightarrow 5$ transition line, along with numerous other important spectral lines from various atomic and molecular species. Furthermore, this frequency range is a focal point for future Event Horizon Telescope (EHT) observations, which aim to produce even higher-resolution images of black holes [1, 2].

Given the limited number of sites on Earth capable of supporting astronomical observations at Band-9, it is crucial to optimise observation time and maximise the scientific output from the few observatories that can operate at these high sub-millimetre frequencies. Key facilities include the James Clerk Maxwell Telescope (JCMT) and the Sub-millimetre Array (SMA), both located at the summit of Mauna Kea on Hawai'i Island; the Greenland Telescope (GLT), if relocated to the summit of Greenland [3]; the South Pole Telescope (SPT) at the Antartica [4]; and the Leighton Chajnantor Telescope (LCT) in the Chilean highlands [5], among others. This frequency range is also relevant to the Atacama Pathfinder Experiment (APEX) telescope's Swedish-ESO PI Instrument for APEX (SEPIA) receiver [6], as well as the ALMA Wideband Sensitivity Upgrade (WSU) programme [7, 8], both of which aim to enhance observational capabilities and expand scientific discoveries in this challenging yet critical domain.

Designing and operating a superconductor-insulator-superconductor (SIS) mixer at Band-9 presents several specific challenges compared to lower frequency bands. The commonly used niobium (Nb) transmission line experiences a significant increase in loss due to Cooper pair breaking above the (2Δ) energy gap of Nb. This energy gap is around 680 GHz, which lies near the centre of the original ALMA-defined Band-9 (602–720 GHz) bandwidth. Additionally, the surface kinetic inductance of the transmission line gradually increases across this frequency range. A further challenge arises when the mixer is driven with sufficient local oscillator (LO) pump power. Under these conditions, the first photon step is partially eroded by the reversed second photon step [9], limiting the available bias voltage range for optimal operation.

While the current ALMA Band-9 mixers have demonstrated exceptional performance [10], enabling numerous significant scientific achievements, there remains scope for further improvement. In addition to the anticipated upgrade of ALMA Band-9 from double sideband (DSB) operation to sideband-separating (2SB) operation [11], potential enhancements include:

Objective #1: Expanding the intermediate frequency (IF) operation bandwidth to 20 GHz, and

Objective #2: Extending the radio frequency (RF) bandwidth from the original 602–720 GHz to the extended 580–740 GHz range [12].

Both objectives are in alignment with the goals of the ALMA WSU programme [7, 8]. As the SIS junction theoretically should be terminated with an IF impedance 3–4× their normal resistance (R_N) [13], maintaining this impedance match over more than 1 or 2 octave of IF frequency range is particularly challenging.

In this study, we aim to investigate whether the aforementioned objectives can be achieved using existing, well-proven superconducting nano-fabrication technologies, thereby avoiding complications to the already successful superconducting device fabrication process. Specifically, we focus on:

- Employing standard AlO_x barrier tunnel junction technology with a full niobium (Nb) transmission line circuit, without relying on exotic superconducting materials such as niobium nitride (NbN) or niobium titanium nitride (NbTiN), or normal metals like gold (Au) or aluminium (Al);
- Using modest critical current density AlO_x tunnel junction technology around 10 kA cm^{-2}, avoiding the need for aluminium nitride (AlN) barriers or high critical current density AlO_x barriers;
- Retaining full Nb junction technology without incorporating NbN or NbTiN electrodes, including hybrid junction technologies [14];
- Eliminating the use of any external IF matching circuit [15], thereby simplifying the mixer block design. This approach is particularly advantageous given the successful implementation of cartridge-style receivers for ALMA, where additional microwave IF matching boards would otherwise increase the mixer block footprint, which is undesirable for high-frequency receivers in array applications;
- Utilising full-height rectangular input waveguides ($160 \times 320\,\mu$m) instead of the current ALMA Band-9 design, which employs half-height rectangular waveguides. This simplification improves machining accuracy and reduces complexity in mixer block fabrication.

The primary goal of this study is to determine how far existing, proven technologies can be optimised to address these challenges before resorting to more advanced, resource-intensive

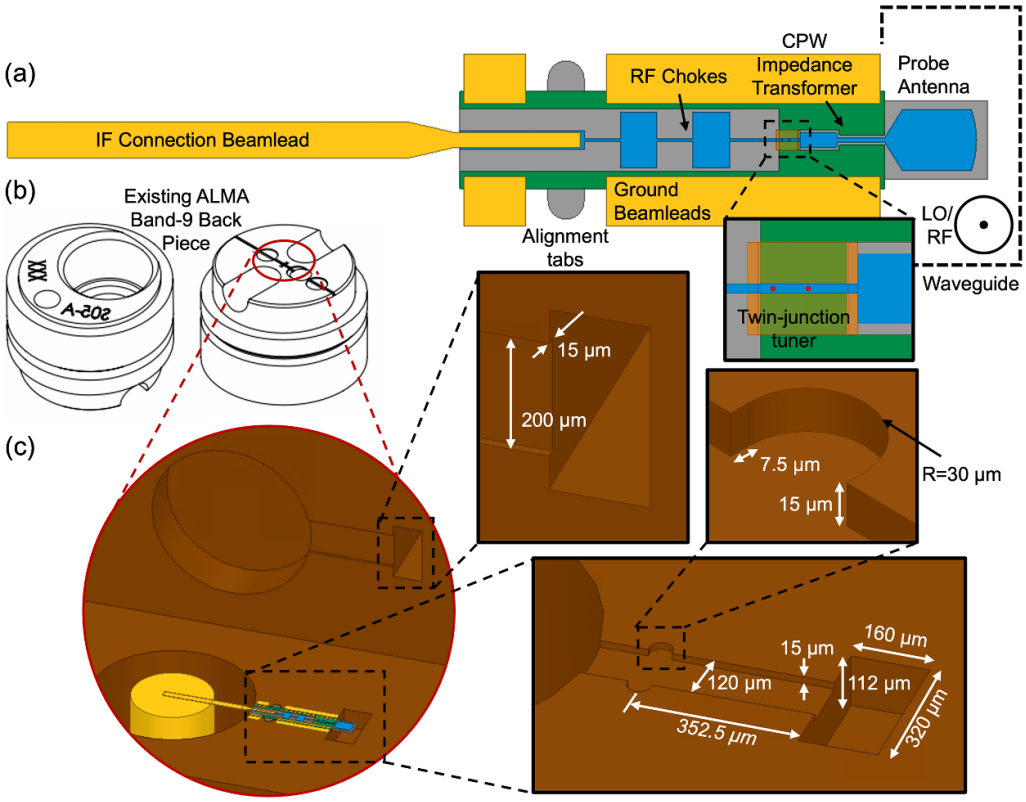

Figure 1. (a) Layout of the SOI mixer chip presented in this paper. The blue-shaded area represents the top 400 nm Nb layer, while the green-shaded area represents the bottom 250 nm ground layer. The length of the proposed SOI mixer chip and the IF connection beam lead are adjusted to fit the layout of the existing ALMA Band-9 back-piece, with modifications to the waveguide dimensions and grooves on both the upper and lower back-piece blocks to accommodate the SOI chip. (b) The original ALMA Band-9 back-piece mixer block designed for quartz mixer chip. See [10] for details. (c) A sketch of the internal structure of the new upper and lower back-piece blocks that needs to be modified to host the SOI mixer chip, showing the dimensions of the waveguide, back-short, grooves, and alignment tab trenches.

solutions that may require significant time and investment to mature.

The development of advanced ALMA-WSU Band-9 receivers requires a concerted effort from multiple areas of expertise to optimise each component in the receiver chain, from the quasi-optical elements to the downstream backend spectrometer. This paper focuses primarily on investigating the theoretical limits of RF and IF performance from the perspective of mixer chip design, aiming to provide a reference for future receiver development in this frequency range. The predicted mixer performance may not fully reflect the actual receiver performance in practical operation, as it depends on several additional factors, such as the availability of impedance-matched wideband IF amplifiers and the corresponding wideband readout spectrometer, broadband and well-matched feedhorns, and high-power stable local oscillator (LO) across the entire RF range.

2. Mixer chip design

Our Band-9 SIS mixers employ a radial-rectangular probe antenna [16, 17], housed within a full-height $160 \times 320\,\mu$m rectangular waveguide, serving as the waveguide-to-planar circuit transition antenna. The mixer chips are fabricated using $10\,\mu$m silicon-on-insulator (SOI) substrate technology [18–20], which facilitates the mounting, alignment, and shaping of the mixer chips. More importantly, the use of SOI technology minimises RF power leakage through the gaps in the trenches hosting the mixer chip. This is particularly advantageous when utilising specific types of on-chip antennas, such as twin-slot [21–23], bow-tie [24, 25], or probe antennas.

Figure 1 illustrates the layout of our mixer design. The niobium (Nb) radial-rectangular probe is supported on a $10\,\mu$m thick SOI substrate. For operation near 650 GHz, the broad-side diameter of the rectangular waveguide is set to $320\,\mu$m, corresponding to a cutoff frequency of approximately 470 GHz. The mixer chip is mounted within a small opening milled across the cross-section of the rectangular waveguide, with a height of $15\,\mu$m. The antenna is suspended $112\,\mu$m above the termination of the rectangular waveguide, forming the backshort. The dimensions of the probe and backshort were optimised using Ansys® High Frequency Structure Simulator (HFSS) [26] to achieve optimal power coupling and bandwidth performance. Additionally, two semi-circular tabs were integrated into the SOI chip design to assist with mounting and alignment. These tabs are particularly important for accurately positioning the probe relative to the rectangular waveguide, as misalignment can significantly impact the bandwidth performance [27].

Figure 1(b) depicts the configuration of our WSU mixer chip, which is based on aluminium oxide (AlO_x) tunnel junctions with a normal-resistance-area (RnA) product of $20\,\Omega{\cdot}\mu m^2$ and a specific capacitance of $80\,fF\,\mu m^{-2}$, corresponding to a critical current density of about $10\,kAcm^2$. This value is modest and conservative given modern cleanroom capabilities, yet it ensures high production yield. To tune out the parasitic capacitance, which would otherwise short the junctions at such high frequencies, we adopt the widely used twin-junction tuner circuit approach [28, 29]. This approach offers superior RF bandwidth performance compared to end-stub or end-loaded tuning circuits [30], which rely on a single tunnel junction and have been shown to exhibit slightly inferior RF bandwidth performance [31]. The junction arrays are embedded in a microstrip transmission line, formed using a 400 nm top and 250 nm ground Nb film sandwiching a 250 nm thick silicon monoxide (SiO) dielectric layer.

The width and length of the narrow microstrip section connecting the two-junction array are optimised to present an inductive load to each junction, thereby broadening the RF bandwidth. An impedance transformer section is incorporated before the tuner circuit to mitigate the impedance mismatch between the output of the probe antenna and the junction array. Additionally, a five-section high-low impedance RF choke is employed after the tuner circuit to prevent RF power leakage into the IF chain. A gold beam lead connects the mixer chip directly to a 50 Ω SMA (SubMiniature version-A) pin directly without any IF matching circuit. To ensure proper grounding, additional beam leads are positioned along the two wide edges of the mixer chip, providing robust grounding to the circuit.

Apart from the characteristics of the junction itself, one of the limiting factors for IF bandwidth performance is the on-chip planar circuit used to achieve broad RF bandwidth and maximise RF coupling to the junction, as described earlier. These ancillary circuits, such as the impedance transformer and the RF choke, are typically realised using microstrip technology due to their well-understood electromagnetic (EM) behaviour, ease of design, and the confined transmission field lines. This is crucial for minimising cross-talk, leakage, and avoiding unwanted on-chip resonances [32]. However, microstrip circuits acting as shunt capacitance in parallel with the junction capacitance inevitably increase the parasitic IF capacitance, which in turn limits the IF bandwidth.

To address this, our WSU mixer design minimise the use of microstrip circuit and replace them with carefully designed coplanar waveguide (CPW) transmission lines, including the probe antenna feed line, the RF impedance transformer, and the RF chokes. Only the tuning circuit comprising the two junctions are connected with microstrip. Extensive EM simulations were then performed using HFSS to ensure that no parasitic behaviours, such as unwanted resonances, leakage, or cross-talk, would affect the RF and IF bandwidth performance of the optimised mixer chip, without altering the setup of the antenna and the waveguide, except for variations in designs with different junction sizes (see section 2.1).

2.1. Naming convention

For clarity and ease of discussion, we first summarise the variations of mixer designs presented in this paper, along with the different sets of noise-bandwidth requirements that will serve as benchmarks for evaluating their performance.

Mixer Design Variations: This study considers three distinct mixer designs, each differing in junction size while maintaining the same overall topology and chip layout. The on-chip circuits, including the probe antenna dimensions, tuning circuit, impedance transformer and rectangular waveguide backshort etc are optimised for best performance in each case:

Design #1: with twin $1.0\,\mu m^2$ AlO_x junctions
Design #2: with twin $0.8\,\mu m^2$ AlO_x junctions
Design #3: with twin $0.6\,\mu m^2$ AlO_x junctions

RF Bandwidth Ranges: Two RF bandwidth ranges are considered in this work:

(i) Existing ALMA-defined Band-9:
- 100% RF bandwidth from 602–720 GHz
- 80% RF bandwidth from 614–708 GHz

(ii) Extended Band-9 range (as proposed by Rearini *et al* [12])
- 100% RF bandwidth from 580–740 GHz
- 80% RF bandwidth from 596–724 GHz

Noise-Bandwidth Requirements: The performance of each mixer design is evaluated against four noise-bandwidth requirements, applicable to both the existing and extended Band-9 ranges:

Existing 100%: 261 K over 100% RF range
Existing 80%: 178 K over 80% RF range
ALMA-WSU 100%: 145 K over 100% RF range
ALMA-WSU 80%: 121 K over 80% RF range

The quoted noise limits are refer to the double sideband (DSB) receiver noise. The single sideband (SSB) value is twice the DSB noise.

3. Heterodyne performance

Once the mixer chip designs (each optimised based on the selected junction size) were finalised using the electromagnetic modelling package to optimise power coupling between the input rectangular waveguide and the tunnel junctions, as well as between the junctions and the IF port in the microwave regime, we evaluated the heterodyne mixing performance of the SIS mixer chip using SuperMix [13, 33], a software package developed based on superconducting quantum mixer theory [34]. The S-parameter matrices of the mixer chip, simulated with HFSS, were exported to SuperMix to form the complete mixer circuit [15].

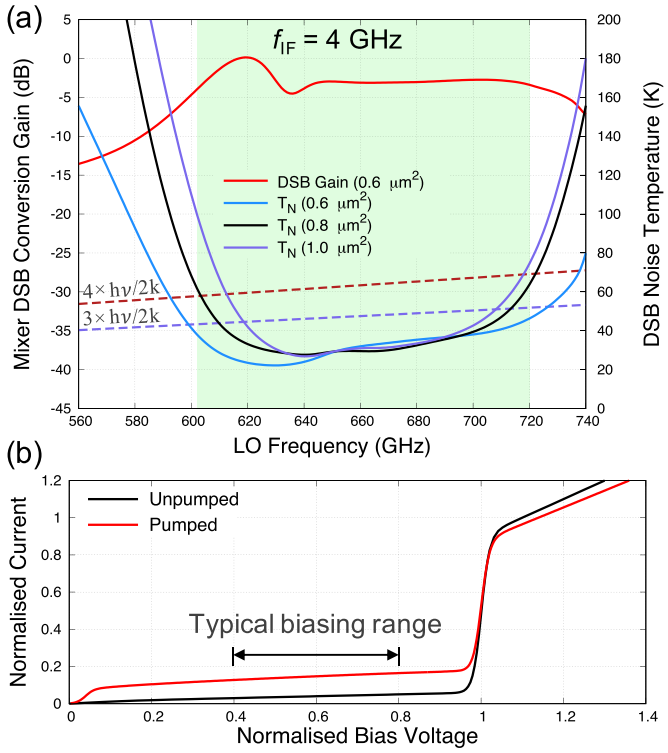

Figure 2. (a) SuperMix predicted heterodyne performance of the optimised mixer designs with 0.6 μm^2, 0.8 μm^2 and 1.0 μm^2 junctions. Note that this simulation is performed with a fixed IF frequency of 4 GHz, with the bias voltage and LO pumping power adjusted at each RF frequency for minimum noise, hence not reflecting the actual operational condition, but simply to give a first-hand idea of the RF bandwidth performance. (b) The theoretical unpumped and pumped (at 700 GHz) normalised IV curve used in SuperMix to simulate the heterodyne performance of the mixers, showing the typical voltage biasing range.

In figure 2(a), we present the predicted double-sideband (DSB) heterodyne performance of the three different optimised mixer designs, based on twin junction sizes of 0.6 μm^2, 0.8 μm^2 or 1.0 μm^2, simulated using the theoretical current–voltage (IV) curve shown in figure 2(b). From these simulation results, we conclude that a junction size of at least 0.8 μm^2 is necessary to cover the entire 602–720 GHz range, assuming a noise temperature less than 4× the DSB quantum limit. Smaller junction sizes tend to widen the RF bandwidth, while larger junctions narrow it.

However, note that figure 2(a) was simulated across the LO frequency range with a fixed IF frequency of 4 GHz. The LO pump power and the junction bias voltage were adjusted for each LO tuning frequency to achieve optimal noise performance. In practice, during observation, the LO does not necessarily need to be set at the extreme ends of the RF band, since the LO frequency depends on the available IF bandwidth of the mixer and backend processor.

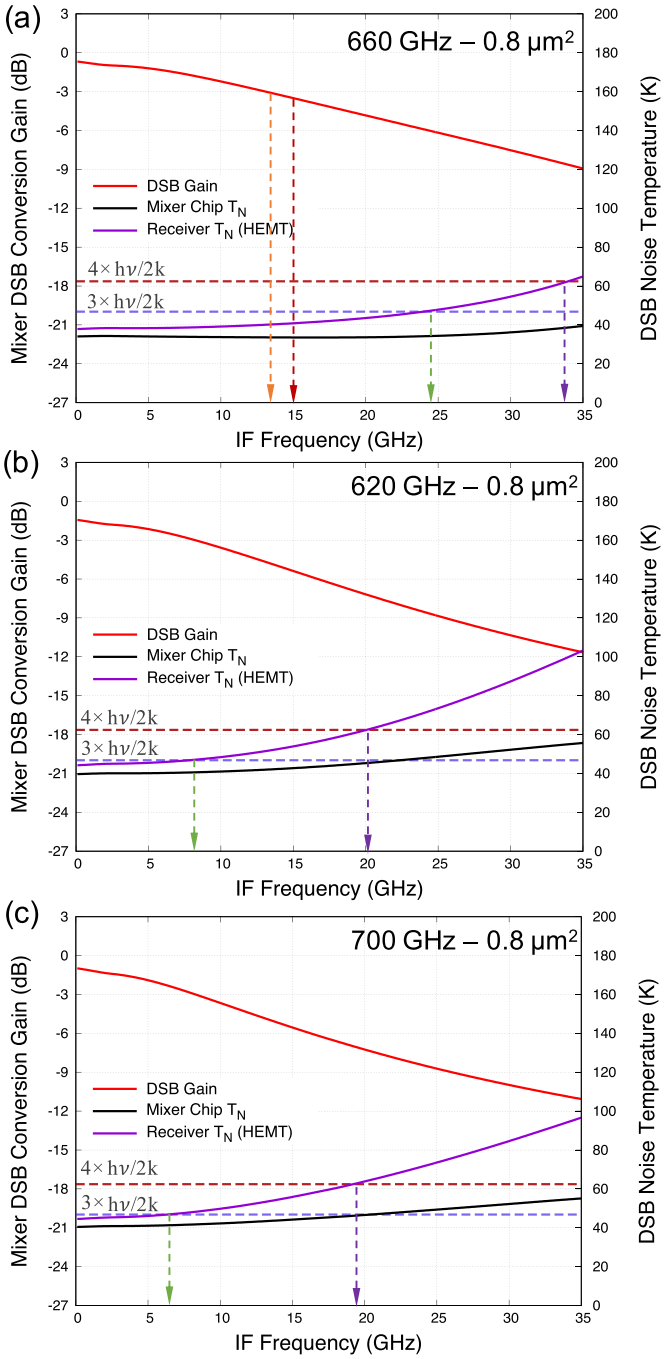

Figure 3. (a) The IF bandwidth performance of the mixer design with 0.8 μm^2 junctions with the LO set at 660 GHz, along with the definition of the differences that can be used to determine the IF bandwidth performance. The dark purple curve shows the receiver noise temperature with the SIS mixer read out with a semiconductor amplifier with an added noise (T_{LNA}) performance fitted to a linear curve where T_{LNA} = 4 K at f_{IF} = 4 GHz and T_{LNA} = 7 K at f_{IF} = 20 GHz [35]. The bias voltage and LO pumping power adjusted to achieve broadest IF bandwidth while avoiding positive conversion gain for operational stability. (b) DSB IF bandwidth performances near the edges of the RF band at 620 GHz and (c) 700 GHz.

3.1. Definition of IF bandwidth

In this section, we focus on the mixer design based on twin 0.8 μm^2 junctions. As shown in figure 3(a), our mixer designs exhibit broad IF bandwidth performance, as we significantly minimise the IF capacitance in the design. However, the definition of the 'IF bandwidth' depends on how it is defined,

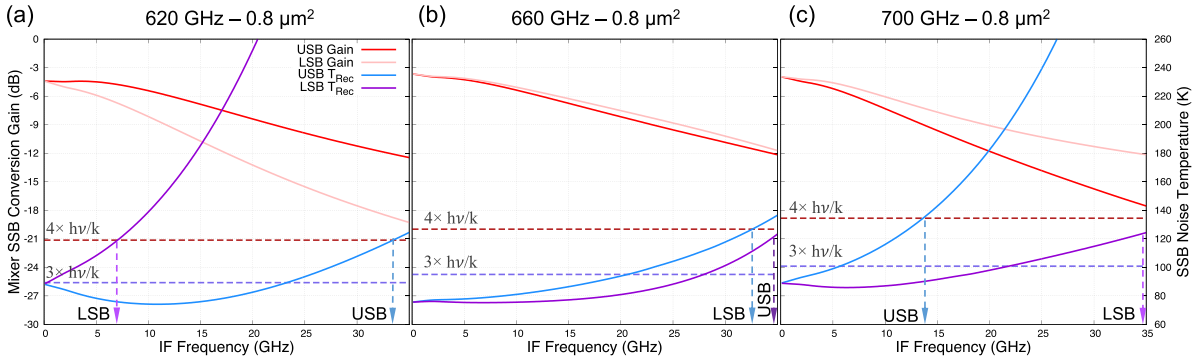

Figure 4. Single sideband gain and noise performances at different LO/RF tunings across the IF bandwidth.

as there is no established convention for this. Some possible definitions, as illustrated in figure 3(a), include:

- The –3 dB DSB gain limit, indicated by the orange dashed line in figure 3(a), resulting in a ∼13 GHz IF bandwidth.
- The –3 dB down from the peak DSB gain, indicated by the dark-red dashed line in figure 3(a), resulting in a near 15 GHz IF bandwidth.
- The receiver noise temperature, accounting for the intrinsic DSB gain and noise performance of the mixer chip readout with a low-noise high electron mobility transistor (HEMT) amplifier ($T_{\rm rec} = T_{\rm SIS} + T_{\rm LNA}/G_{\rm SIS}$), where $T_{\rm LNA}$ is emulated as a linear projection from $T_{\rm LNA} = 4$ K at $f_{\rm IF} = 4$ GHz to $T_{\rm LNA} = 7$ K at $f_{\rm IF} = 20$ GHz. The noise temperature crossing 3× the DSB quantum limit, indicated by the green dashed line in figure 3(a), results in a close to 24.5 GHz IF bandwidth.
- The same as above, but referenced to 4× the DSB quantum limit, indicated by the dark purple dashed line in figure 3(a), resulting in a close to 34 GHz IF bandwidth.

For our investigations in this paper, we adopt option 4 as the reference for defining the IF bandwidth. It is clear that reducing the noise temperature of the readout amplifier would improve IF performance, bringing it closer to the intrinsic noise performance of the mixer itself, which could extend the IF bandwidth beyond the 35 GHz range in all cases. However, it is challenging to develop an actual LNA that is well impedance matched across such broad frequency range. The various parasitic reactances also increase with higher IF frequencies, hence it may not be realistic to operate the receive beyond 20 GHz IF bandwidth.

If we assume a 20 GHz IF bandwidth based solely on figure 3(a) for design cases, then as shown in the purple curve of figure 2(a), it appears feasible to cover the entire 602–720 GHz range with a noise temperature of less than 4× the DSB quantum limit, even with the 1.0 μm^2 junction design. This would involve only three LO tunings: at 620 GHz for the 600–640 GHz range, 660 GHz for the 640–680 GHz range, and 700 GHz for the 680–720 GHz range[4].

However, as shown in figures 3(b) and (c), the IF bandwidth does not remain constant across the chosen RF/LO driving points. The IF bandwidth narrows near the edges of the RF band. While the intrinsic noise temperature of the mixer remains relatively flat across the IF frequency range, the DSB gain decreases more rapidly, thereby narrowing the receiver noise bandwidth. Although the performance near the edges is not as optimistic as that at the centre of the RF band, but they are still close to 20 GHz IF bandwidth for the 0.8 μm^2 junction case. But the same may not be true for the other designs. This highlights the challenge of defining the IF bandwidth in such cases, as the bandwidth depends on the specific RF/LO frequency. Therefore, we argue that a more appropriate way to describe the RF and IF bandwidth is to fully assess the single sideband (SSB) receiver noise performance under the operational LO tuning conditions during observations, particularly to evaluate sensitivity near the edges of the RF band.

3.2. *Double sideband vs single sideband operation analysis*

To complicate matters further, not only does the DSB receiver noise temperature increase near the edges of the band, but the DSB gain is also an average product of the folded upper sideband (USB) and lower sideband (LSB) gains. These gains do not necessarily behave symmetrically, and the single sideband (SSB) IF bandwidth performance presents a drastically different picture near the edges of the band, as shown in figure 4. Hence, the IF definition using a DSB performance may not reflect the actual reality for a sideband separating (2SB) operation, especially near the edges of the band where the sideband ratio (SBR) worsen. Notice how the poorer performance of the USB and LSB swaps at the lower and upper RF/LO operating points, which is not ideal for our operation. This is

[4] Here, we assume a low-noise amplifier (LNA) with a DC–20 GHz operational bandwidth. However, most LNAs do not operate efficiently at ultra-low IF frequencies, so there will be gaps near the LO tuning frequencies. As a result, more than three tunings would be needed to cover the entire RF bandwidth.

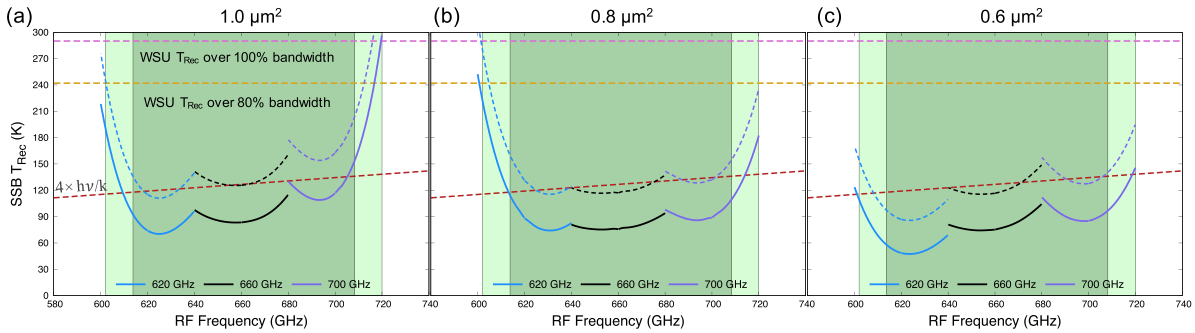

Figure 5. The SuperMix simulation resembles the actual operation of the SIS mixer, illustrating both the operational RF coverage and the IF bandwidth performance. The light green shaded area represents the 100% RF bandwidth defined by the existing ALMA specification, spanning from 602 to 720 GHz, while the dark green shaded area indicates 80% of this defined bandwidth. The solid line curves depict the receiver's SSB noise temperature with the linear-fit $T_{\rm LNA}$, assuming no RF optical losses. In contrast, the dashed line curves represent the receiver's SSB noise temperature with the linear-fit $T_{\rm LNA}$, but with 10% warm (297 K) RF optical losses. The pink and orange horizontal dashed lines correspond to the receiver noise temperature requirements specified by the ALMA-WSU programme for 100% and 80% RF bandwidth, respectively.

not surprising, as sideband performance is primarily determined by the RF power coupling to the chip and the junctions. Therefore, it is essential to examine the SSB performance carefully, rather than assuming that the DSB performance will be replicated across the RF bandwidth. We believe this is the most reliable way to estimate the performance of an actual sideband separating (2SB) mixer.

It is easier to observe the effect if we plot the actual LO tuning biasing points anticipated during observation. This is shown in figure 5, where we observe that the LSB at the lower frequency end (620 GHz) deteriorates much faster than the USB, and vice versa for the USB at the higher frequency end (700 GHz). Nevertheless, we can see that the performance of even the 1.0 μm^2 junction design is satisfactory, where we successfully cover both the 80% and 100% RF bandwidth requirements defined by the latest ALMA WSU project [7].

To better estimate the actual receiver performance, figure 5 includes scenarios where the receiver experiences 10% warm optics losses (at room temperature, 297 K), in addition to the added noise of the LNA. These are represented by the dashed curved lines in the plot. As can be seen, even with a significant warm optics loss, our 1.0 μm^2 junctions design nearly covers the entire WSU 100% bandwidth requirement, missing it by just a few GHz. However, it certainly meets the 80% WSU bandwidth requirement throughout. With smaller junction sizes (0.6 and 0.8 μm^2), we are able to cover the entire existing Band-9 RF bandwidth with only three LO tunings, hence achieving our first objective i.e. to extend the IF bandwidth to 20 GHz while meeting the WSU noise temperature requirement across the original Band-9 range.

4. Extended RF bandwidth requirement

In this section, we investigate whether our Band-9 mixer designs are capable of covering the extended Band-9 range from 580–740 GHz suggested by Rearini *et al* [12]. To cover the wider RF bandwidth, four LO tunings would be required instead of three, assuming a 20 GHz IF bandwidth. This operational mode, using the exact same mixer designs previously discussed, is shown in figure 6. Similar to section 3.2, in the following analysis, we refer to a more realistic receiver noise performance that accounts for LNA added noise and 10% warm optic losses.

The first key observation is that, using the original ALMA Band-9 receiver noise temperature specification as a guideline (355 K and 522 K SSB $T_{\rm rec}$ for 80% and 100% bandwidth respectively), we can extend slightly beyond the originally defined bandwidth (602–720 GHz), with the 1.0 μm^2 junction design, by employing just four LO tunings. In this configuration (figure 6(a)), the in-band performance from the original ALMA-defined Band-9 bandwidth (602–720 GHz) also shows slight improvements when we utilise only the USB at $f_{\rm LO} = 610$ GHz and the LSB at the $f_{\rm LO} = 710$ GHz settings. But the 1.0 μm^2 junction design is unable to cover the entire extended Band-9 range from 580–740 GHz. Nevertheless, using the same $T_{\rm rec}$ specification, both the 0.8 and 0.6 μm^2 designs successfully cover the extended Band-9 range from 580–740 GHz.

Using the more stringent sensitivity requirements specified by the WSU programme as reference (242 K and 290 K SSB $T_{\rm rec}$ for 80% and 100% bandwidth respectively), all three design variations managed to cover the existing 602–720 GHz range, again achieving our first objective i.e. to extend the IF bandwidth to 20 GHz while meeting the WSU noise temperature requirement across the original Band-9 range.

To meet the same WSU requirement across the extended 580–740 GHz range, only the 0.6 μm^2 junctions design managed to achieve our second objective i.e. to extend the IF bandwidth to 20 GHz while meeting the WSU noise temperature requirement across the extended Band-9 range. However, the 0.8 μm^2 junction design comes close to meeting the WSU requirements across the extended Band-9 range, falling short by just a few GHz near the edges of the band. These results are summarised in the table shown in figure 7.

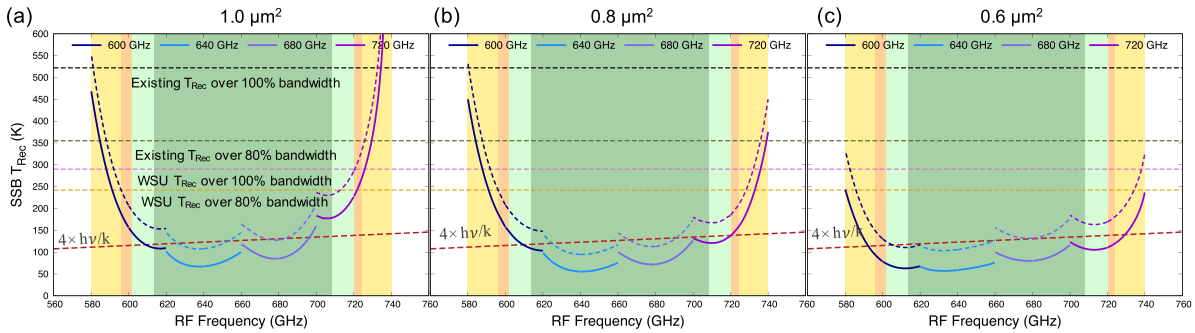

Figure 6. The RF and IF bandwidth performance of the optimised mixer designs with four LO tunings, covering the extended Band-9 RF frequency range. The light green shaded area represents the 100% RF bandwidth defined by the existing ALMA specification, ranging from 602–720 GHz, while the dark green shaded area corresponds to 80% of this defined bandwidth. The yellow shaded area indicates the 100% RF bandwidth for the extended Band-9 range, spanning from 580–740 GHz, with the orange shaded area representing 80% of this extended bandwidth. The solid line curves depict the receiver's SSB noise temperature with the linear-fit T_{LNA}, assuming no RF optical losses. In contrast, the dashed line curves represent the receiver's SSB noise temperature with the linear-fit T_{LNA}, but with 10% warm (297 K) RF optical losses. The specified receiver noise temperatures for both existing and WSU requirement, at both 100% and 80% bandwidth, are shown as horizontal dashed lines with different colours.

Design #1: 1.0 μm square junctions		RF Range (GHz)	Receiver Noise Requirement			
			Existing 100%	Existing 80%	WSU 100%	WSU 80%
			522 K	355 K	290 K	242 K
Existing Band-9 range	80%	614 – 708		✓		✓
	100%	602 – 720	✓		✓	
Extended Band-9 range	80%	596 – 724		✓		✗
	100%	580 – 740	✗		✗	

Design #2: 0.8 μm square junctions		RF Range (GHz)	Receiver Noise Requirement			
			Existing 100%	Existing 80%	WSU 100%	WSU 80%
			522 K	355 K	290 K	242 K
Existing Band-9 range	80%	614 – 708		✓		✓
	100%	602 – 720	✓		✓	
Extended Band-9 range	80%	596 – 724		✓		✓
	100%	580 – 740	✓		✗	

Design #3: 0.6 μm square junctions		RF Range (GHz)	Receiver Noise Requirement			
			Existing 100%	Existing 80%	WSU 100%	WSU 80%
			522 K	355 K	290 K	242 K
Existing Band-9 range	80%	614 – 708		✓		✓
	100%	602 – 720	✓		✓	
Extended Band-9 range	80%	596 – 724		✓		✓
	100%	580 – 740	✓		✓	

Figure 7. Tables showing which noise-bandwidth criteria each mixer design could meet. The table was made using the performance of each mixer designs shown in figure 6, referring to the receiver's SSB noise temperature with the linear-fit T_{LNA}, and a 10% warm (297 K) RF optical losses (dashed curves), as reference.

5. Other practical considerations

So far, our focus has primarily been on the RF and IF bandwidth performance of the SIS mixer chips, evaluated based on their heterodyne performance (conversion gain and noise temperature) to assess their potential for meeting the WSU requirements. However, several important practical considerations remain unaddressed, some of which fall beyond the scope of this paper. These include operational stability, the impact of fabrication tolerances, and the availability of suitable wideband LNAs and wideband backend spectrometer etc. In this section, we briefly highlight a few of these issues. For a more detailed discussion of these and other design considerations, we refer the reader to [13].

5.1. Operational stability

An SIS mixer may experience gain instability when the conversion gain is too high and/or the RF return loss ($S_{11,\mathrm{RF}}$) is greater than approximately −6 dB. To partially mitigate this issue, in earlier analyses, we select the bias voltage and LO pumping level to avoid positive conversion gain while maintaining low noise performance. However, as shown in figure 8, the return loss performance of the 1.0 μm^2 junction design remains better than −6 dB only within the 612–700 GHz range, while the 0.8 μm^2 junction design maintains this performance from approximately 610–708 GHz. This suggests that outside these ranges, these mixers may experience operational instability near the band edges. Nevertheless, this issue may be less severe in practice, as the conversion gain

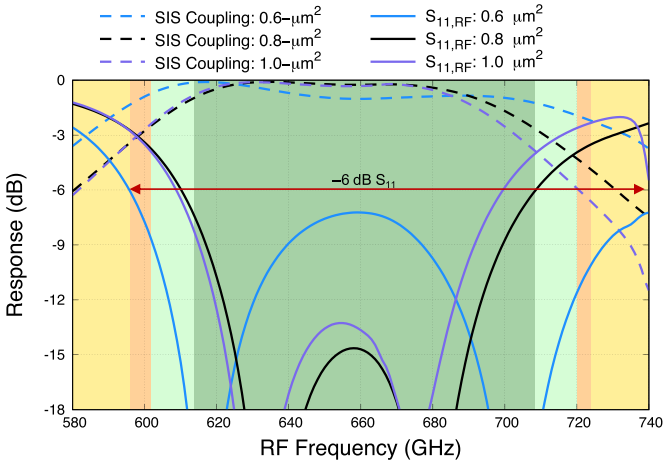

Figure 8. The total RF power coupling to the SIS junctions (dashed curves) and the return loss $S_{11,RF}$ performance (solid curves) of all three designs with 0.6, 0.8 and 1.0 μm^2 junctions.

Design #1: 1.0 μm square junctions		RF Range (GHz)	Receiver Noise Requirement			
			Existing 100%	Existing 80%	WSU 100%	WSU 80%
			522 K	355 K	290 K	242 K
Existing Band-9 range	80%	614 – 708		✓		✓
	100%	602 – 720	✗		✗	
Extended Band-9 range	80%	596 – 724		✗		✗
	100%	580 – 740	✗		✗	

Design #2: 0.8 μm square junctions		RF Range (GHz)	Receiver Noise Requirement			
			Existing 100%	Existing 80%	WSU 100%	WSU 80%
			522 K	355 K	290 K	242 K
Existing Band-9 range	80%	614 – 708		✓		✓
	100%	602 – 720	✗		✗	
Extended Band-9 range	80%	596 – 724		✗		✗
	100%	580 – 740	✗		✗	

Design #3: 0.6 μm square junctions		RF Range (GHz)	Receiver Noise Requirement			
			Existing 100%	Existing 80%	WSU 100%	WSU 80%
			522 K	355 K	290 K	242 K
Existing Band-9 range	80%	614 – 708		✓		✓
	100%	602 – 720	✓		✓	
Extended Band-9 range	80%	596 – 724		✓		✓
	100%	580 – 740	✗		✗	

Figure 9. Tables showing which noise-bandwidth criteria each mixer design could meet if we consider the $S_{11,RF} \leqslant -6$ dB requirement to avoid potential instability issue. The table was made using the performance of each mixer designs shown in figure 6, referring to the receiver's SSB noise temperature with the linear-fit T_{LNA}, and a 10% warm (297 K) RF optical losses (dashed curves), as reference.

tends to drop rapidly at the band edges, which helps to dampen unwanted instability.

Conversely, the smaller 0.6 μm^2 junction design achieves $S_{11,RF} \leqslant -6$ dB over a broader range, from 595–740 GHz, covering nearly the entire extended Band-9 range except at the lowest few frequencies. While the 0.6 μm^2 junction design does not achieve the ultimate WSU noise-bandwidth product over the extended Band-9 range (objective #2), it successfully meets the ALMA-WSU requirement over the existing Band-9 bandwidth (objective #1). Based on this, we therefore conclude that to minimise operational issues, the development of a mixer design should focus on the twin 0.6 μm^2 junction configuration. To reflect these additional considerations, we update the table in figure 7 to exclude frequency ranges where instability may occur, with the table shown in figure 9.

5.2. *Practical IF amplifiers*

Theoretically, SIS mixers achieve optimal IF performance when terminated with a load resistance of approximately 3–4× their normal junction resistance (R_N). In this manuscript, we assume an ideal IF amplifier with perfect impedance matching to a 50 Ω environment. While it is possible to design a custom non-50 Ω LNA to better match this requirement, we have not assume such an integration in this study, as it could be challenging to achieve this over the broad IF bandwidth.

In reality, if an ultra-wideband 50 Ω IF LNA may not achieve perfect input (S_{11}) impedance matching, it could lead to standing waves between the SIS mixer chip and the IF amplifier, thereby affecting mixer performance. Investigating the impact of imperfect impedance matching over such a broad IF bandwidth is beyond the scope of this paper. However,

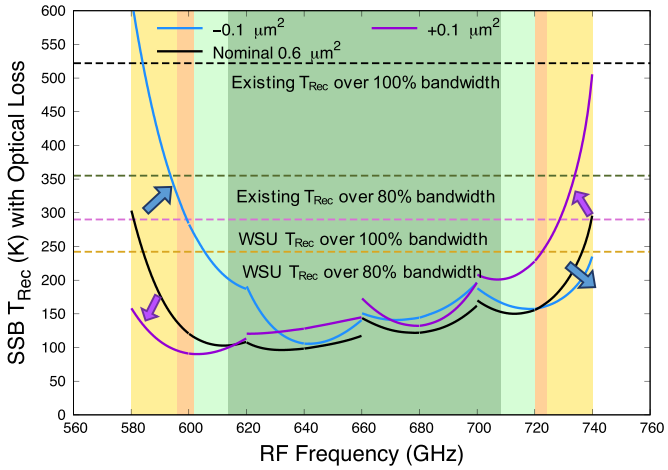

Figure 10. The simulated receiver noise temperature including the linear-fit $T_{\rm LNA}$, 10% warm (297 K) RF optical losses for the 0.6 μm^2 junctions design, showing the bandwidth performance of the mixer design should the tunnel junction size is varied by $\pm$0.1 μm^2. The design is marginal, if the performance is referred to ALMA-WSU sensitivity requirement over the extended RF bandwidth, but still managed to cover the updated WSU sensitivity over the original Band-9 bandwidth.

we hope this work provides valuable guidance for IF amplifier developers in optimising the Band-9 WSU receiver in the near future. If achieving wideband impedance matching in an LNA proves challenging, an alternative solution would be to use a broadband isolator between the mixer chip and the LNA to mitigate mismatch effects. While not an ideal approach, it could serve as a practical workaround.

5.3. Junction size tolerance analysis

Next, we examine the effect of junction size variation on the performance of our Band-9 mixers: figure 10. For this analysis, we use the 0.6 μm^2 junctions design, though the general behaviour is consistent across the other two designs. If the junctions are fabricated larger than anticipated, the tuned RF bands shift towards the lower frequency end, while maintaining a similar bandwidth product. Conversely, if the junctions are smaller than expected, the RF bandwidth narrows and shifts towards the higher frequency end. Despite these variations, our 0.6 μm^2 junction design can still meet the 80% and 100% WSU sensitivity requirements over the original ALMA-defined RF bandwidth of 602–720 GHz, although it falls short for the extended RF bandwidth. With modern electron-beam lithography techniques, we are confident that a junction size tolerance of $\pm$0.1 μm^2 is achievable.

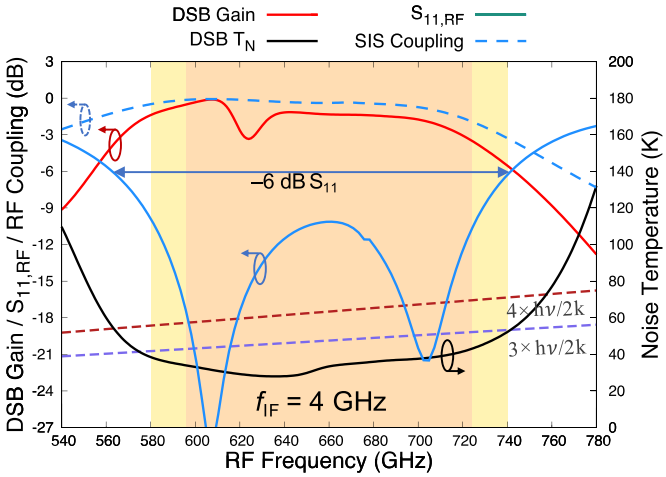

(a)

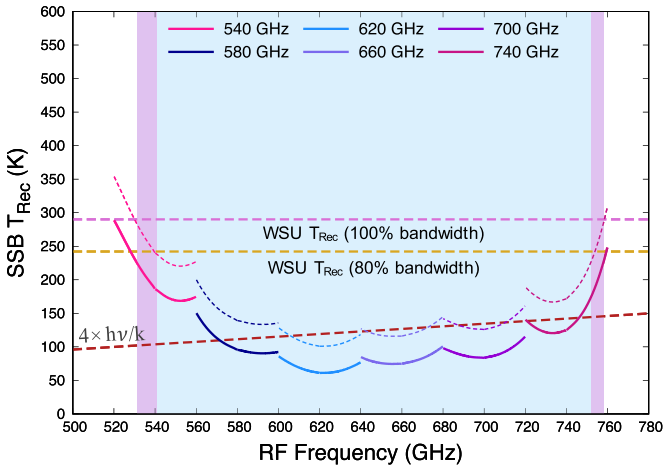

(b)

Figure 11. (a) SuperMix predicted DSB gain and noise temperature performance for the optimised mixer designs with a twin 0.5 μm^2 AlN junction tuner circuit, simulated using the same theoretical IV curve shown in figure 2(b). The dashed blue curves shows the total RF power coupling from the input waveguide to the junctions and the solid blue curve the return loss performance. (b) The RF and IF bandwidth performance of the optimised AlN mixer designs with six LO tunings, covering an extended Band-9 RF frequency range. The solid line curves depict the receiver's SSB noise temperature with the linear-fit $T_{\rm LNA}$, assuming no RF optical losses. In contrast, the dashed line curves represent the receiver's SSB noise temperature with the linear-fit $T_{\rm LNA}$, but with 10% warm (297 K) RF optical losses. The receiver noise temperature requirements for WSU, at both 100% and 80% bandwidth, are indicated by horizontal dashed lines in different colours. The light-blue shaded area indicates the bandwidth where the SSB noise temperature with optical losses falls below the WSU 80% bandwidth requirement, and the light-purple shaded area shows the bandwidth where the SSB noise temperature with optical losses is below the WSU 100% bandwidth requirement.

6. Improved performance with AlN sub-micron junctions

Finally, we investigate the potential improvement in bandwidth performance for these Band-9 mixers by relaxing the stringent requirements outlined in section 1, specifically:

- Replacing the AlO_x barrier tunnel junction with AlN junction technology, and
- Utilising half-height rectangular input waveguides (80×320 μm) to reduce the input waveguide impedance, thereby broadening the RF bandwidth.

For this investigation, we use half-micron AlN tunnel junctions with an RnA product of $20\,\Omega{\cdot}\mu\mathrm{m}^2$ and a specific capacitance of 55 fF $\mu\mathrm{m}^{-2}$, as reported in [36]. The mixer chip layout follows the previous designs, with optimisations made to the probe dimensions and on-chip circuit components to maximise RF bandwidth performance. As shown in figure 11, these modifications enable the AlN mixer's intrinsic DSB noise temperature to cover the full extended Band-9 RF range from 580–740 GHz, with a DSB noise temperature satisfying $T_N < 3 \times h\nu/2k$ and $S_{11,\mathrm{RF}} \leqslant -6$ dB from 560–740 GHz.

The predicted SSB receiver noise temperature, excluding optical losses, extends further from 528–758 GHz, with reference to the WSU 80% noise temperature requirement. Factoring in the 10% optical losses, the RF bandwidth remains within similar range from 540–754 GHz, requiring only six LO tunings if the SSB receiver noise temperature requirement is relaxed to meet the WSU 100% noise temperature guideline. This represents a 35% bandwidth coverage at near-THz frequency range. Although such broad RF bandwidth coverage in the vicinity of Band-9 may not be practical for ground-based observations, it could be of significant value for future far-infrared balloon missions [37–39] or space missions [40–45].

7. Conclusion

This study demonstrates that our WSU Band-9 SIS mixer designs, based on conventional AlO_x tunnel junctions, can achieve wide IF bandwidth performance as dictated by the WSU requirement. Our detailed electromagnetic simulations and noise performance analysis performed using quantum mixing theory show that the mixer design with $0.6\,\mu\mathrm{m}^2$ junctions provides good sensitivity performance, meeting the ALMA-WSU 80% and 100% RF bandwidth requirements, across the existing ALMA Band-9 (602–720 GHz) frequency range. However, to fully cover the extended Band-9 range (580–740 GHz) with similar 20 GHz IF bandwidth performance would require half-micron AlN junction technology.

Data availability statement

All data that support the findings of this study are included within the article (and any supplementary files).

Acknowledgments

This research was funded in part by the European Commission Horizon-Infra-2022-Tech-01 RadioBlock project and the UK-STFC Small Award 2024 Grant (ST/Y002210/1). The D.Phil. studentship of J-H Kim is supported by the STFC studentship, Oxford's Mansfield College Jocelyn Bell-Burnell Scholarship, and the Oxford Clarendon Scholarship. For the purpose of Open Access, the author has applied a CC BY public copyright licence to any Author Accepted Manuscript version arising from this submission.

ORCID iDs

B-K Tan 0000-0002-6252-9351
F Boussaha 0000-0002-7611-0148

References

[1] Roelofs F, Fromm C M, Mizuno Y, Davelaar J, Janssen M, Younsi Z, Rezzolla L and Falcke H 2021 Black hole parameter estimation with synthetic very long baseline interferometry data from the ground and from space *Astron. Astrophys.* **650** A56
[2] Patel N *et al* 2023 Planned upgrades on the Greenland Telescope for the Next Generation Event Horizon Telescope observations *American Astronomical Society Meeting Abstracts* vol 55 pp 305–16
[3] Chen M-T *et al* 2023 The Greenland Telescope—Construction, Commissioning and Operations in Pituffik *Publ. Astron. Soc. Pac.* **135** 095001
[4] Carlstrom J E *et al* 2011 The 10 meter south pole telescope *Publ. Astron. Soc. Pac.* **123** 568
[5] Lyu F, Du W, Shi W and Zhang Y 2023 Design and performance analysis of NbN-based SIS mixer in the 750–950 GHz frequency band for LCT telescope *Proc. SPIE* **12617** 1891–6
[6] Belitsky V *et al* 2018 SEPIA–a new single pixel receiver at the APEX telescope *Astron. Astrophys.* **612** A23
[7] Asayama S *et al* 2020 Report of the ALMA front-end & digitizer requirements upgrade working group *ALMA Report* ALMA Observatory
[8] Carpenter J, Brogan C, Iono D, and Mroczkowski T 2022 The ALMA2030 wideband sensitivity upgrade (arXiv:2211.00195)
[9] Tan B-K, Yassin G, Grimes P, Leech J, Jacobs K and Groppi C 2011 A 650 GHz unilateral finline SIS mixer fed by a multiple flare-angle smooth-walled horn *IEEE Trans. Terahertz Sci. Technol.* **2** 40–49
[10] Baryshev A M *et al* 2015 The ALMA Band 9 receiver-design, construction, characterization and first light *Astron. Astrophys.* **577** A129
[11] Khudchenko A, Hesper R, Baryshev A, Gerlofma G, Barkhof J, Adema J, Mena P, Klapwijk T and Spaans M 2012 Sideband separating mixer for 600-720 GHz for ALMA band 9 upgrade *Proc. SPIE* **8452** 313–9
[12] Realini S, Hesper R, Barkhof J and Baryshev A 2024 ALMA Band 9 upgrade: a feasibility study *EPJ Web Conf.* **293** 00043
[13] Rice F R 2020 *A Very Wide Bandwidth SIS Heterodyne Receiver Design for Millimeter and Submillimeter Astronomy* (California Institute of Technology)
[14] Khudchenko A, Baryshev A M, Rudakov K I, Dmitriev P M, Hesper R, de Jong L and Koshelets V P 2015 High-gap Nb-AlN-NbN SIS junctions for frequency band 790–950 GHz *IEEE Trans. Terahertz Sci. Technol.* **6** 127–32
[15] Tan B-K, Yassin G and Grimes P 2014 Ultra-wide intermediate bandwidth for high-frequency SIS mixers *IEEE Trans. Terahertz Sci. Technol.* **4** 165–70
[16] Withington S, Leech J, Yassin G, Isaak K G, Jackson B D, Gao J R and Klapwijk T M 2001 A 350GHz radial-probe SIS mixer for astronomical imaging arrays *Int. J. Infrared Millim. Waves* **22** 1305–12
[17] Kooi J W, Chattopadhyay G, Withington S, Rice F, Zmuidzinas J, Walker C and Yassin G 2003 A full-height waveguide to thin-film microstrip transition with exceptional RF bandwidth and coupling efficiency *Int. J. Infrared Millim. Waves* **24** 261–84

[18] Kaul A B, Bumble B, Lee K A, LeDuc H G, Rice F and Zmuidzinas J 2004 Fabrication of wide-IF 200–300 GHz superconductor–insulator–superconductor mixers with suspended metal beam leads formed on silicon-on-insulator *J. Vac. Sci. Technol. B* **22** 2417–22
[19] Westig M P, Jacobs K, Stutzki J, Schultz M, Justen M and Honingh C E 2011 Balanced superconductor–insulator–superconductor mixer on a 9 μm silicon membrane *Supercond. Sci. Technol.* **24** 085012
[20] Tan B-K, Yassin G, Grimes P and Jacobs K 2013 650 GHz SIS mixer fabricated on silicon-on-insulator substrate *Electron. Lett.* **49** 1273–5
[21] Zmuidzinas J and LeDuc H G 1992 Quasi-optical slot antenna SIS mixers *IEEE Trans. Microw. Theory Tech.* **40** 1797–804
[22] Zmuidzinas J, Ugras N G, Miller D, Gaidis M, LeDuc H G and Stern J A 1995 Low-noise slot antenna SIS mixers *IEEE Trans. Appl. Supercond.* **5** 3053–6
[23] Chattopadhyay G, Miller D, LeDuc H G and Zmuidzinas J 2000 A dual-polarized quasi-optical SIS mixer at 550 GHz *IEEE Trans. Microw. Theory Tech.* **48** 1680–6
[24] Shan W, Shi S, Matsunaga T, Takizawa M, Endo A, Noguchi T and Uzawa Y 2007 Design and development of SIS mixers for ALMA band 10 *IEEE Trans. Appl. Supercond.* **17** 363–6
[25] Kojima T, Kroug M, Takeda M, Shan W, Fujii Y, Uzawa Y, Wang Z and Shi S 2009 Performance of terahertz waveguide SIS mixers employing epitaxial NbN films and Nb junctions *IEEE Trans. Appl. Supercond.* **19** 405–8
[26] Ansys, Inc 2025 Ansys engineering simulation software (available at: www.ansys.com/en-gb)
[27] Tan B-K, Rudakov K, Koshelets V P, Khudchenko A, Baryshev A M and Yassin G 2022 Comparing the performance of 850 GHz integrated bias-tee superconductor-insulator-superconductor (SIS) mixers with single-and parallel-junction tuner *Supercond. Sci. Technol.* **35** 125008
[28] Zmuidzinas J, LeDuc H G, Stern J A and Cypher S R 1994 Two-junction tuning circuits for submillimeter SIS mixers *IEEE Trans. Microw. Theory Tech.* **42** 698–706
[29] Belitsky V Y, Jacobsson S W, Filippenko L V and Kollberg E L 1995 Broadband twin-junction tuning circuit for submillimeter SIS mixers *Microw. Opt. Technol. Lett.* **10** 74–78
[30] Kooi J W 2008 Advanced receivers for submillimeter and far infrared astronomy *PhD Thesis* University of Groningen
[31] Kim J-H, Chaumont C, Boussaha F and Tan B-K 2025 Band-combining SIS mixer designs for the Africa Millimetre Telescope *34th Int. Symp. on Space Terahertz Technology*
[32] Shan W, Ezaki S, Kaneko K, Miyachi A, Kojima T and Uzawa Y 2019 Experimental study of a planar-integrated dual-polarization balanced SIS mixer *IEEE Trans. Terahertz Sci. Technol.* **9** 549–56
[33] Ward J, Rice F, Chattopadhyay G and Zmuidzinas J 1999 SuperMix: a flexible software library for high-frequency circuit simulation, including SIS mixers and superconducting elements *Proc. 10th Int. Symp. on Space Terahertz Technology* pp 269–81
[34] Tucker J R and Feldman M J 1985 Quantum detection at millimeter wavelengths *Rev. Mod. Phys.* **57** 1055
[35] López-Fernández I, Gallego-Puyol J D, Diez C, Malo-Gomez I, Amils R I, Flückiger R, Marti D and Hesper R 2024 A 16-GHz bandwidth cryogenic IF amplifier with 4-K noise temperature for sub-mm radio-astronomy receivers *IEEE Trans. Terahertz Sci. Technol.* **14** 336–45
[36] Pavolotsky A, Kojima T, Masui S and Belitsky V 2022 SIS technology development to serve Next Generation receivers for ALMA *Proc. 32nd IEEE Int. Symp. on Space THz Technology (ISSTT 2022)* pp 16–20
[37] Pineda J L *et al* 2019 The far-infrared astronomy stratospheric balloon facility *Bull. Am. Astron. Soc.* **51** 7–177
[38] Goldsmith P F 2023 Stratospheric Balloon Missions for High Resolution Submillimeter-FIR Astronomical Spectroscopy *2023 48th Int. Conf. on Infrared, Millimeter and Terahertz Waves (IRMMW-THz)* (IEEE) pp 1–2
[39] Udinski E and Hamilton A 2024 NASA balloon program overview *JAXA and Hiroshima University Collaboration Meetings*
[40] Silva J R *et al* 2024 High-resolution receiver for the single aperture large telescope for Universe studies *J. Astron. Telesc. Instrum. Syst.* **10** 042308–042308
[41] Rigopoulou D *et al* 2021 The far-infrared spectroscopic surveyor (FIRSS) *Exp. Astron.* **51** 699–728
[42] Wiedner M C, Baryshev A, Grimes P and Tan B 2024 Concept study of the Heterodyne Spectroscopy Instrument (HSI) for the proposed Far-IR Spectroscopy Space Telescope (FIRSST) *Proc. 34th IEEE Int. Symp. on Space THz Technology* (National Radio Astronomy Observatory)
[43] Rigopoulou D *et al* 2022 The far-infrared spectroscopic surveyor: probing role of the interstellar medium in star formation and galaxy evolution *Proc. SPIE* **12180** 121802G
[44] Rigopoulou D *et al* 2016 The Far Infrared Spectroscopic Explorer (FIRSPEX): probing the lifecycle of the ISM in the Universe *Proc. SPIE* **9904** 850–6
[45] Mehdi I *et al* 2019 Far-infrared heterodyne array receivers *Bull. Am. Astron. Soc.* **51** id–120